Desalination and Water Treatment
www.deswater.com

doi: 10.5004/dwt.2017.20272

65 (2017) 367–374
February

Synthesis and characterization of amino-functionalized magnetic nanocomposite (Fe_3O_4–NH_2) for fluoride removal from aqueous solution

Abbas Norouzian Baghani[a], Amir Hossein Mahvi[b], Noushin Rastkari[c], Mahdieh Delikhoon[d], Sara Sadat Hosseini[e], Razieh Sheikhi[f,*]

[a]*Center for Water Quality Research (CWQR), Institute for Environmental Research (IER), Tehran University of Medical Sciences, Tehran, Iran, Tel. +989102141053; Fax: +98 21 88950188; email: Abbas.jj.norozi@gmail.com*
[b]*Center for Solid Waste Research, Institute for Environmental Research (IER), Tehran University of Medical Sciences, Tehran, Iran, Tel. +989123211827; Fax: +98 21 88950188; email: ahmahvi@yahoo.com*
[c]*Center for Air Pollution Research (CAPR), Institute for Environmental Research (IER), Tehran University of Medical Sciences, Tehran, Iran, Tel. +989122261013; Fax: +98 21 88950188; email: nr_rastkari@yahoo.com*
[d]*Department of Occupational Health Engineering, School of Public Health, Shiraz University of Medical Sciences, Shiraz, Iran, Tel. +989165186550; email: Mdelikhon@yahoo.com*
[e]*Department of Environmental Health Engineering, School of Public Health, Tehran University of Medical Sciences, Tehran, Iran, Tel. +989122450195; Fax: +98 21 88950188; email: ssa_hosseiny@yahoo.com*
[f]*School of Public Health, Tehran University of Medical Sciences, Tehran, Iran, Tel. +989124390149; Fax: +98 21 88950188; email: sheikhi@tums.ac.ir*

Received 30 May 2016; Accepted 16 October 2016

ABSTRACT

Paramagnetic nanoparticles (Fe_3O_4–NH_2) were prepared by simply treating the Fe_3O_4 nanoparticles with 1,6-hexanediamine at 198.8°C, and the defluoridation ability of the resulted nanoparticles (Fe_3O_4–NH_2) was evaluated. The synthesized sorbent was verified by scanning electron microscope, transmission electron microscope, X-ray powder diffractometer, and vibrating sample magnetometer. Besides, various factors such as pH, contact time, temperature, initial concentration, and sorbent dosage that influenced the efficiency of fluoride ions removal were evaluated. The equilibrium data were studied using Langmuir and Freundlich isotherms. The best interpretation for the adsorption of fluoride ions was found to follow the Langmuir isotherm, and the maximum adsorption capacity was 52.91 mg g^{-1} at pH = 2 and 313°K. In addition, the adsorptive properties of Fe_3O_4–NH_2 were extremely pH dependent. Adsorption of fluoride ions attained equilibrium within 30 min, and the best sorbent dose was observed to be 0.4 g/L. The maximum fluoride removal was found to be 76.8% at the best conditions. Finally, the adsorption mechanism studies revealed that the adsorption of fluoride ions on Fe_3O_4–NH_2 could be related to electrostatic attraction.

Keywords: Fluoride removal; Amino-functionalized magnetic nanocomposite; Langmuir isotherm; Adsorption; 1,6-hexanediamine

1. Introduction

Fluoride contamination in drinking water has been recognized as one of the major problems worldwide because of natural and anthropogenic emission [1,2]. Throughout the world, fluoride compounds are employed in industry for a wide range of applications, such as aluminum production, glass fiber, phosphate fertilizers, bricks, tiles, ceramics, drinking water fluoridation, and toothpaste [3]. Review of the literature indicated that long-term ingestion of high-fluoride drinking water could lead to fluorosis, which is a chronic disease manifested through mottling of the teeth in

* Corresponding author.

mild cases, softening of bones, ossification of tendons and ligaments [4,5], and neurological damage in severe cases [6]. A large proportion of the population in North Africa, China, and India suffers from fluoride poisoning [6,7]. Experiences from different parts of the globe show that different techniques are used for water defluoridation [8]. The most commonly used methods for water defluoridation include adsorption [1,6,8–16], ion exchange [17], and precipitation [8]. Adsorption is one of the most dominant methods because of its simplicity and availability of a wide range of adsorbents [1]. Among the sorbents thought to be useful for defluoridation, amino-functionalized magnetic nanocomposite (Fe_3O_4–NH_2) is better because of its low cost, lack of secondary wastes (without sludge generation), availability, higher defluoridation capacity, and fast separation for large volumes of solutions [18]. In addition, Fe_3O_4–NH_2 has a lot of amino-groups that can be used as chelation sites and electrostatic attraction. Therefore, an amino-group on the surface of Fe_3O_4 nanoparticles is able to adsorb cations and anions in water and wastewater [18–25]. Moreover, it is usually difficult to segregate adsorbents from large volumes of solutions rapidly, while Fe_3O_4–NH_2 can solve this problem since it can be easily separated from the solution by an external magnetic field [20].

Based on what was mentioned above, we aimed to find an efficient, reliable, and simple method to quickly separate adsorbents [24] from aquatic solutions. Thus, we prepared Fe_3O_4–NH_2 as a practical approach for fluoride removal process and the adsorbent was characterized by transmission electron microscope (TEM), X-ray powder diffractometer (XRD), vibrating sample magnetometer (VSM), and scanning electron microscope (SEM). The majority of magnetic nanoparticles have been used for removal of heavy metals, but we used Fe_3O_4–NH_2 for the first time for removal of anions, particularly fluoride ions. Finally, fluoride adsorption isotherms by Fe_3O_4–NH_2 were analyzed.

2. Materials and methods

2.1. Synthesis of amine-functionalized magnetic nanoparticles (Fe_3O_4–NH_2)

All the necessary chemicals that were used in this study were of analytical grade with further purification, and were purchased from Merck Co. (Germany). All aqueous solutions were prepared by using double distilled water. Besides, the magnetic nanoparticles (MNPs) modified with 1,6-hexanediamine were synthesized by 1.0 g $FeCl_3 \cdot 6H_2O$ as a single iron source in 30 mL ethylene glycol followed by adding 4.0 g of anhydrous sodium acetate and 1,6-hexanediamine (3.6 g) as nitrogen source and were stirred vigorously to make a transparent solution. Finally, this solution was moved into a Teflon-lined autoclave and was continuously reacted at 198.8°C for 8 h. The product was washed with water and ethanol for 3 times to remove the ethylene glycol and redundant 1,6-hexanediamine effectively. Also, the product was isolated from various solvents by using a permanent handheld magnet during each step and was then dried in a vacuum oven at 50°C to gain the black powder. This black powder abbreviated as Fe_3O_4–NH_2 was originally prepared by Wang et al. [24].

2.2. Characterization

The purity of the amine-functionalized MNPs was confirmed by a number of techniques. The morphology of Fe_3O_4–NH_2 was studied using a field emission SEM (ZEISS, Germany) and TEM images that were determined using a field emission TEM (Tecnai F20, USA). Besides, the crystal structure of Fe_3O_4–NH_2 was measured by X'Pert PRO (Philips, Holland) using Cu Kα radiation (λ = 0.1541 nm) ranging from 20° to 70° (2θ) at 30 kV and 30 mA. The paramagnetic properties of Fe_3O_4–NH_2 were also investigated at room temperature by the magnetization curve measured by using a VSM (LDJ 9600, LDJ Electronics Company of USA). Finally, the concentration of fluoride ions in the solutions was measured by a spectrophotometer DR/5000 (Method 8029).

2.3. Fluoride ions adsorption

First, the fluoride solutions were prepared. Sodium fluoride (NaF) was used to prepare the fluoride stock solution. Then, fluoride solution 100 mg/L followed by 3, 5, and 7 mg/L solutions were made from the stock solution. Afterward, it was important to determine the best conditions. In doing so, 50 ml water samples containing fluoride and a specific amount of nanoparticles, as the absorbent, were poured into Erlenmeyer flasks. To determine the best pH, the samples' pH was adjusted in acidic, basic, and neutral ranges until the effects of several pH levels on fluoride removal were specified. It was found that fluoride was removed at acidic pH (pH = 2). Therefore, first, the level of pH was adjusted at the best level, and then, the samples were placed on a reciprocating shaker (model 3018GFL) at different speeds, times, and adsorbent dosages. Then, the best speed of shaker, retention time, and adsorbent dosage were determined. After that, the effect of Fe_3O_4–NH_2 on the removal of fluoride from water samples was investigated. Finally, the best conditions for fluoride removal were applied at 3, 5, and 7 mg/L fluoride concentrations. In each experiment, pH of the sample was adjusted, and 20 mg of Fe_3O_4–NH_2 in 50 ml of the sample solution was applied for a specified reaction time. After that, Fe_3O_4–NH_2 was deposited using a magnet, and the supernatant was removed from the flask. Finally, the fluoride concentration was measured using a spectrophotometer DR/5000 (Method 8029). The detection limit was 0.02–2 mg/LF^-.

3. Results and discussion

3.1. Characterization of Fe_3O_4–NH_2

3.1.1. Particle size and morphology

The morphology of NH_2–Fe_3O_4 was studied by TEM. The TEM image of NH_2–Fe_3O_4 has been illustrated in Fig. 1(a). The NH_2–Fe_3O_4 prepared in this study was multidispersed with an average diameter of around 35 nm. It is known that magnetic particles of less than 30 nm show parmagnetism [26]. This suggests that these nanoparticles can be easily dispersed into aqueous solutions as adsorbents, which is attributed to addition of amino groups on the surfaces of Fe_3O_4 nanoparticles [27]. The SEM image presented in Fig. 1(b) reveals that the size of the synthesized NH_2–Fe_3O_4 was less than 100 nm. The image also shows that the size of NH_2–Fe_3O_4 was much

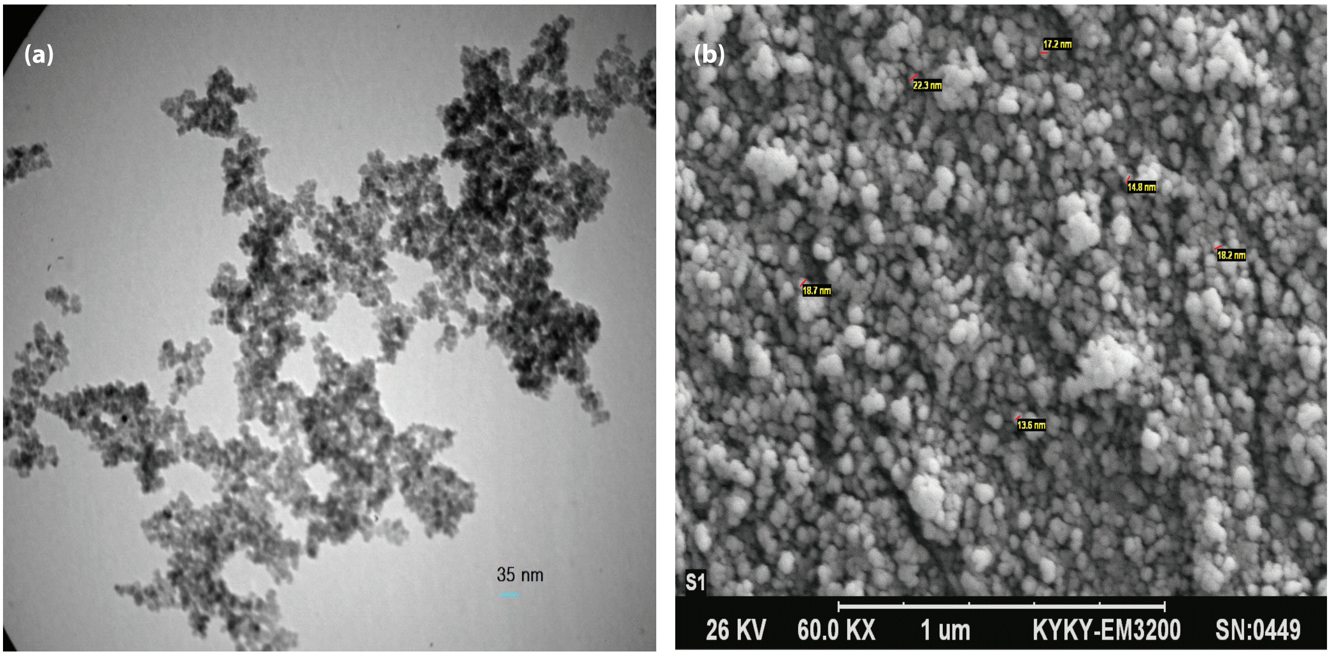

Fig. 1. (a) TEM image of Fe_3O_4–NH_2 and (b) SEM image of Fe_3O_4–NH_2.

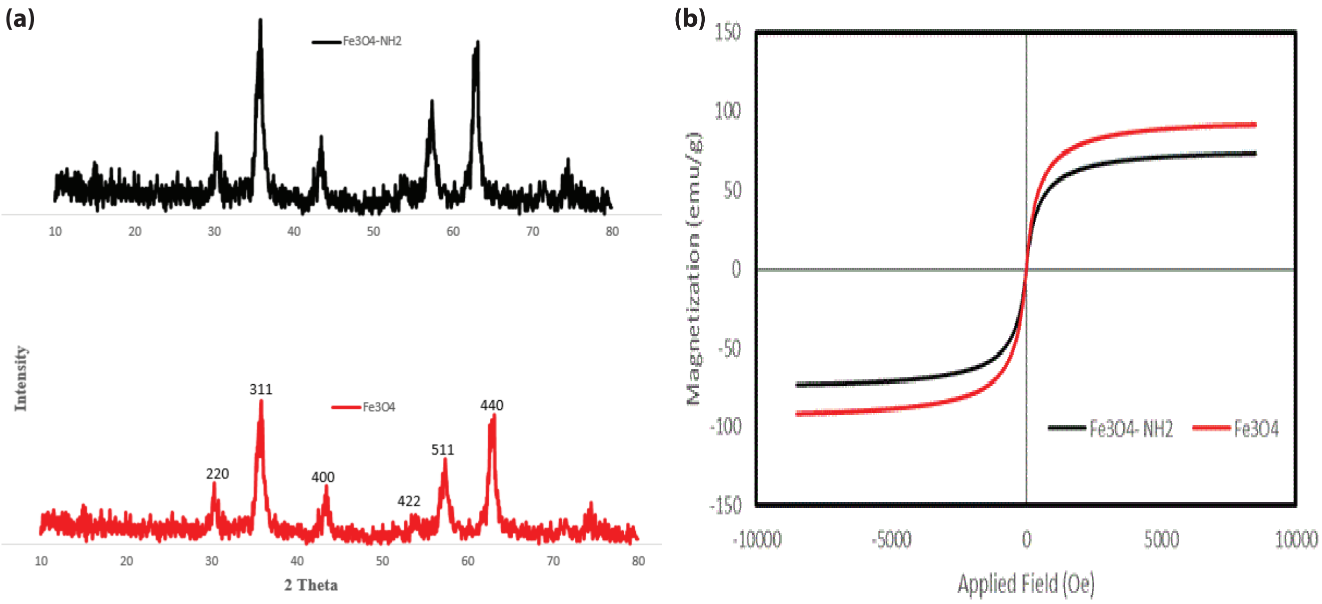

Fig. 2. (a) XRD image of Fe_3O_4–NH_2 and (b) VSM image of Fe_3O_4–NH_2.

smaller compared with the naked particles, proving the coating of 1,6-hexanediamine [18].

3.1.2. X-ray powder diffractometer

The crystalline structure of NH_2–Fe_3O_4 was verified by XRD, as shown in Fig. 2(a) [28]. The XRD pattern of NH_2–Fe_3O_4 showed the six characteristic peaks of Fe_3O_4 at about 2θ = 30.1°, 35.5°, 43.1°, 53.4°, 57.0°, and 62.6° corresponded to their intensity indices (220, 311, 400, 422, 511, and 440, respectively). This indicated that amino groups did not cause significant changes in the phase property of Fe_3O_4 cores and that NH_2 occurred only on the surface of the Fe_3O_4 cores, which is in accordance with the reports by Wang et al. [24] and Zhao et al. [25]. Moreover, the strong and sharp peaks proved that NH_2–Fe_3O_4 was well crystallized.

3.1.3. Vibrating sample magnetometer

The plots of magnetization vs. magnetic field (M–H loop) for NH_2–Fe_3O_4 were assessed by employing VSM at room temperature, and the results have been shown in Fig. 2(b) [28].

The M–H curves showed that NH_2–Fe_3O_4 was essentially superparamagnetic, and NH_2–Fe_3O_4 had magnetization saturation (Ms) value of 77.32 emu g^{-1}. Besides, MNPs showed superparamagnetic property with Ms value of 90.43 emu/g^{-1} [18]. This result suggested that decrease in Ms might be associated with increased mass of $-NH_2$ on the surface of Fe_3O_4. Moreover, the results illustrated in Fig. 3 revealed that NH_2–Fe_3O_4 could be completely separated from the aqueous solution with an external magnetic field within 30 s [28]. Therefore, NH_2–Fe_3O_4 could be regarded as a potential candidate for practical application.

3.2. The effect of various parameters on the adsorption process of fluoride ions

3.2.1. The effect of pH, adsorbent dose, contact time, and different initial concentrations on the removal of fluoride ions

Generally, pH is the most important parameter that influences the adsorption process. To find the best pH for maximum removal of fluoride by NH_2–Fe_3O_4, the experiments were conducted at pH of 2–9 by keeping other parameters constant (initial concentration = 3 mg/L, NH_2–Fe_3O_4 dose = 0.4 g/L, and shaker speed = 200 rpm). Based on the results, the removal of fluoride was decreased from pH 2 to 9 (76.8% to 30%), and the maximum adsorption (76.8%) was gained at pH = 2. pH value affected the adsorption efficiency due to its influence on the amino groups modified on the surface of Fe_3O_4–NH_2. Moreover, the effect of the solution's pH and concentration on the adsorption of fluoride onto Fe_3O_4–NH_2 was investigated by varying the initial concentrations of fluoride at 3, 5, and 7 mg L^{-1}. The effects of solution's pH and concentration on the adsorption of fluoride on Fe_3O_4–NH_2 have been depicted in Fig. 4(a). Accordingly, the adsorption capacity decreased when pH increased from 2.0 to 9.0 because of the decrease in the amount of fluoride adsorbed per unit mass of the adsorbent. In fact, the amount of adsorbed fluoride decreased from 5.76 to 2.25, 8.05 to 2.625, and 9.852 to 2.94 mg g^{-1} at the fluoride concentrations of 3, 5, and 7 mg L^{-1}, respectively. Therefore, the maximum adsorption of fluoride ions occurred at pH = 2. Moreover, adsorption of fluoride ions depended on protonation or deprotonation of functional groups on the surface of Fe_3O_4–NH_2.

Fig. 3. Demonstration of magnetic separation at 30 s.

The pH_{zpc} for Fe_3O_4–NH_2 was 5.8. Therefore, at pH < 5.8, the surface charge of Fe_3O_4–NH_2 was positive, and the electrostatic interactions between fluoride ions and the adsorbent enhanced [18]. The protonation/deprotonation reactions of the amino groups of Fe_3O_4–NH_2 in the solution have been shown in Eq. (1):

$$R - NH_2 + H^+ \leftrightarrow R - NH^{3+} \text{ (amino protonate)} \quad (1)$$

This could be attributed to the fact that under acidic conditions (at pH = 2), amino groups (NH_2) are easily protonated to $-NH^{3+}$, and electrostatic attraction takes place between $-NH^{3+}$ and F^- [21,23,25,29–32].

A scheme for the binding and amino-functionalization procedure of NH_2–Fe_3O_4 and the presumed mechanism of adsorption of fluoride on NH_2–Fe_3O_4 has been shown in Fig. 4(b).

Adsorbent dose is an important parameter that affects fluoride removal efficiency. In the current study, the adsorbent dose ranged from 0.2 to 2 g/L. The initial fluoride ion concentration was fixed at 3 mg/L, and the contact time was

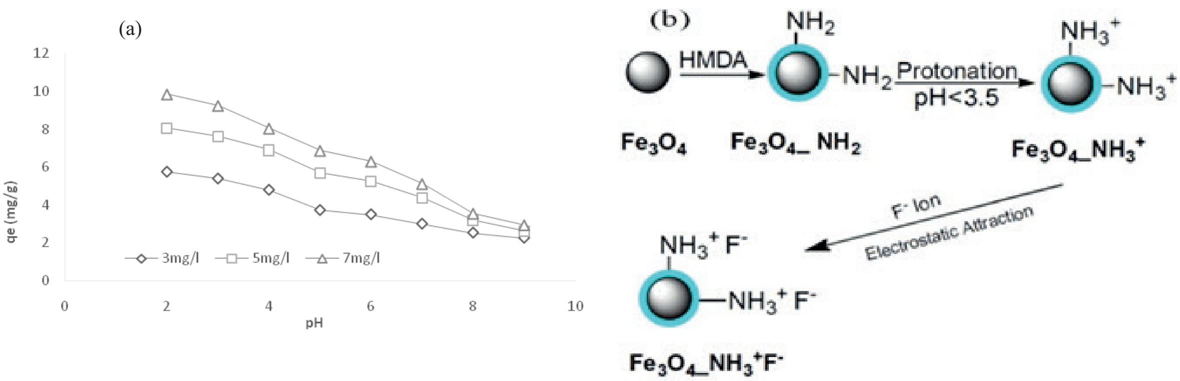

Fig. 4. (a) The effect of solution's pH and concentration on the adsorption of fluoride from aqueous solution by Fe_3O_4–NH_2 and (b) a scheme for the binding and amino-functionalization of Fe_3O_4–NH_2.

held as 30 min, while pH was kept at 2. The results showed that NH_2–Fe_3O_4 was efficient for removal of 50.6% and 52.7% of fluoride ions at the adsorbent doses of 0.2 and 2 g/L, respectively. In addition, the results demonstrated that the best adsorbent dose was 0.4 g/L for fluoride concentration of 3 mg/L, giving 76.8% fluoride ion removal efficiency. Hence, adsorbent dose of 0.4 g/L was chosen for further studies. Overall, the results indicated that the removal of fluoride decreased with increasing the adsorbent dose.

Considering the effects of different contact times (from 10 to 120 min) on fluoride removal while keeping other parameters constant (adsorbent dose = 0.4 g/L, fluoride concentration = 3 mg/L, pH = 2, and stirring rate = 200 rpm), adsorption of fluoride increased with increase in contact time up to 30 min. However, further rise in contact time did not increase the fluoride adsorption process due to deposition of fluoride ions on the available adsorption sites on NH_2–Fe_3O_4. Therefore, the adsorption of fluoride was 76.8% in the best conditions (adsorbent dose = 0.4 g/L, fluoride concentration = 3 mg/L, pH = 2, and stirring rate = 200 rpm) after 30 min. In other words, the remaining fluoride concentration in the aqueous solution was below 1 mg/L that was within the permissible limit suggested by World Health Organization (WHO); i.e., 1–1.5 mg/L [33]. Hence, 30 min was chosen as the contact time at 298°K.

This study assessed the effects of different initial fluoride concentrations (3.0–7.0 mg/L) at the adsorbent dose of 0.4 g/L, pH of 2, stirring rate of 200 rpm, and contact time of 30 min at 298°K. The results disclosed that the removal of fluoride decreased with increase in the initial fluoride ion concentration because the capacity of the adsorbent is consumed slowly with the increase in the initial fluoride concentration. The removal rates of fluoride at the initial concentrations of 3, 5, and 7 mg L^{-1} were 76.8%, 64.4%, and 56.3%, respectively. In addition, the remaining concentrations of fluoride in the aqueous solution were 0.67, 1.61, and 3.06 mg L^{-1} at 3, 5, and 7 mg L^{-1} fluoride concentrations, respectively. Thus, the remaining concentrations increased with increase in the initial fluoride concentration. This could be attributed to the fact that the total available adsorption sites (–NH_2) are limited for a fixed adsorbent dosage and become saturated at a certain concentration. Thus, increase in the initial fluoride ion concentration was accompanied by decrease in the removal percentage. Similar trends have also been reported for fluoride removal by activated charcoal and eggshell powder [34,35].

4. Adsorption model

The equilibrium adsorption capacity for each adsorbent, q_e (mg g^{-1}), can be calculated using Eq. (2) [36]. Adsorption isotherm data are commonly fitted to Langmuir (Eq. (3)) and Freundlich (Eq. (5)) models [31,36]. In this equation, b and q_m are the Langmuir constants, which are related to the apparent heat change and the maximum adsorption capacity, respectively. In the Langmuir model, the form or characteristics of the isotherm can be employed to portend the favorability of the adsorption process under given experimental conditions. The essential characteristics of the isotherm can be shown by a dimensionless constant separation factor, R_L, which has been described in Eq. (4) [37]. In the Freundlich isotherm, K_F [(mg g^{-1}) (mg L^{-1})]$^{1/n}$ and n are the constants, which are related to an indicator of the adsorption capacity and a characteristic coefficient related to the adsorption intensity, respectively [31,36]. The relevant equations for kinetic studies, adsorption capacity, and separation factor (R_L) have been shown in Table 1.

The constant of the Langmuir isotherm and the value of R_L have been summarized in Table 2. Accordingly, the value of R_L at all temperatures was between 0 and 1. Therefore, adsorption was favorable. In addition, the results presented in Fig. 5(a) demonstrated that the experimental data of Fe_3O_4–NH_2 at all temperatures corresponded well to the Langmuir isotherm equation because the correlation coefficients were >0.9204 at all temperatures (R^2 = 0.9204, 0.9676, and 0.9815 for 298°K, 303°K, and 313°K, respectively). The maximum fluoride sorption capacity of NH_2–Fe_3O_4 was found to be 52.91 mg/g at 313°K. Besides, q_m values increased with increase in temperature (Table 2).

The correlation coefficients ($R^2 > 0.92$) and R_L ($0 < R_L < 1$) proved that the Langmuir isotherm fitted better for adsorption of fluoride on NH_2–Fe_3O_4. Langmuir isotherm was depicted with $1/C_e$ vs. $1/q_e$ as shown in Fig. 5(a). Considering the constants of the Langmuir isotherm, q_m values were found to be 22.52, 47.39, and 52.91 at 298°K, 303°K, and 313°K,

Table 1
The isotherm equations and separation factors used for adsorption of fluoride onto Fe_3O_4–NH_2

Eq. (2)	Langmuir isotherm	$\frac{1}{q_e}=\left(\frac{1}{bq_m}\right)\frac{1}{C_e}+\frac{1}{q_m}$	[31,36]
Eq. (3)	Freundlich isotherm	$Q_e = K_F C_e^{\frac{1}{n}}$	[31,36]
Eq. (4)	Equilibrium adsorption capacity	$q_e=\frac{\left(C_0-C_e\right)V}{m}$	[31,36]
Eq. (5)	Separation factor (R_L)	$R_L = 1/(1+bC_O)$	[37]

Note: If: $R_L > 1$, the adsorption is unfavorable; $R_L = 1$, the adsorption is linear; $0 < R_L < 1$, the adsorption is favorable; and $R_L = 0$, the adsorption is irreversible [37].
If: $1/n < 1$, the adsorption is favorable, and $1/n > 1$, the adsorption is unfavorable [31–36].
q_e (mg/g), q_m (mg/g), K_p (mg/g $min^{-0.5}$), C_0 (mg /L), V (mL), m (mg), n (Freundlich constant), b (L mg^{-1}), and K_F [(mg g^{-1}) (mg L^{-1})]$^{1/n}$.

Table 2
Isotherm parameters of fluoride adsorption by Fe_3O_4–NH_2

Langmuir model					Freundlich model			
Temp. (K)	q_{max} (mg g^{-1})	b (L mg^{-1})	R^2	R_L	K_F (mg g^{-1}) (L mg^{-1})$^{1/n}$	R^2	n	$1/n$
293	22.523	0.089	0.9204	0.789	1.47	0.9014	0.9228	1.08
303	47.393	0.045	0.9676	0.8810	1.28	0.8593	0.5784	1.72
313	52.91	0.046	0.9815	0.8787	1.40	0.8331	0.6991	1.43

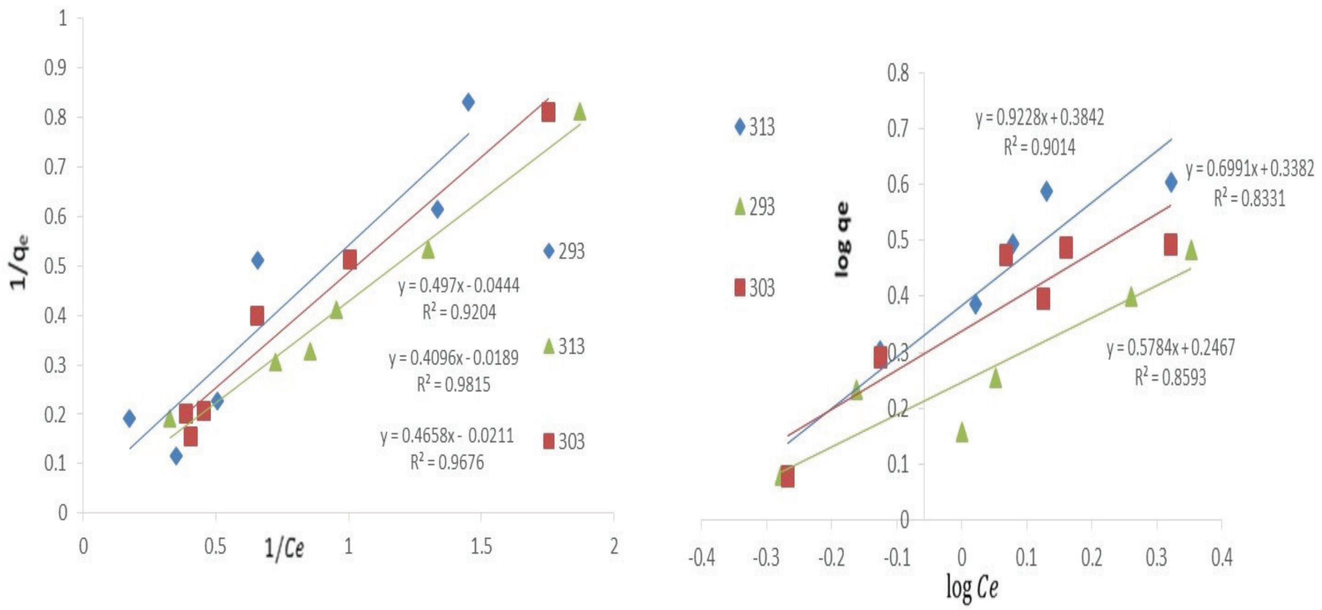

Fig. 5. (a) Langmuir and (b) Freundlich isotherms for adsorption of fluoride.

respectively. Besides, b values were obtained as 0.089, 0.045, and 0.046 at 298°K, 303°K, and 313°K, respectively. Moreover, the values of $1/n$ presented in Table 2 were more than 1. Thus, the adsorption was unfavorable. The Freundlich isotherm was depicted with logq_e vs. logC_e, as shown in Fig. 5(b). Accordingly, K_F values were 1.47, 1.28, and 1.40 at 298°K, 303°K, and 313°K, respectively. Additionally, $1/n$ values were 1.08, 1.72, and 1.43 at 298°K, 303°K, and 313°K, respectively. The experimental data of Fe_3O_4–NH_2 did not well correspond to the Freundlich isotherm equation at all temperatures because the correlation coefficients were <0.9014 (R^2 = 0.9014, 0.8593, and 0.8331 at 298°K, 303°K, and 313°K, respectively).

4.1. *Comparison of adsorption capacity of NH_2–Fe_3O_4 with other adsorbents*

Comparison of the adsorption capacity of Fe_3O_4–NH_2 fitted with Langmuir isotherm with other adsorbents for removal of fluoride has been summarized in Table 3. It is difficult to compare this adsorbent with other adsorbents due to different applied experimental conditions. Yet, removal of fluoride by NH_2–Fe_3O_4 had a much higher maximum adsorption capacity compared with other adsorbents. This can be attributed to the role of amino groups in the adsorption process of fluoride in aqueous solutions. In fact, increase of nitrogen percentage in Fe_3O_4–NH_2 can cause an increase in the value of q_m. Therefore, because of high adsorption capacity and simple preparation of NH_2–Fe_3O_4, it can be used for the removal of fluoride from water and wastewater.

4.2. *Material stability desorption and reusability of Fe_3O_4–NH_2*

Considering the practical application, the sorption/desorption cycle was repeated for 5 times using the same nanoparticles. In addition, each sorption/desorption process experienced a base and a heat treatment [15,28]. According to the results, leaching of the sorbent components in the treated water was undesirable. In order to evaluate the effect of time on leaching of NH_2–Fe_3O_4, 50 mg NH_2–Fe_3O_4 laden with fluoride (after testing under acidic condition sat pH < 3), which was re-suspended in 50 mL deionized water, and the supernatant was measured for Fe concentrations for 6 d. The insignificant leaching of the material components of NH_2–Fe_3O_4 has been presented in Table 4.

5. Conclusions

In the present study, magnetic Fe_3O_4–NH_2 was synthesized via one-pot method for the removal of fluoride ions from aqueous solutions and was characterized by SEM, TEM, XRD, and VSM. According to the results, binding and amino-functionalization did not cause significant changes

Table 3
Comparison of fluoride adsorption capacity of Fe_3O_4–NH_2 and other adsorbents

Adsorbents	Capacity q_m (mg g^{-1})	pH	T (K)	Adsorption isotherm	Refs.
Bark of babul	1.891	8	293	Langmuir	[38]
Eggshell powder	1.09	6.0	303	Langmuir	[35]
PPy/Fe_3O_4 nanocomposites	17.6–22.3	6.5	298–318	Langmuir–Freundlich	[9]
Fe_3O_4@Al(OH)$_3$	88.48	6.5	298	Langmuir	[6]
PURAL®MG-20	5.62	5–7	305 ± 2	Langmuir	[12]
Activated carbon	2.5	3.5	293	Langmuir	[13]
Activated charcoal	$q_e = 0.462C_e / (1 + 0.429C_e)$	2	–	Langmuir	[38]
$KMnO_4$ modified carbon	15.9	2.0	298	–	[39]
Acid treated spent bleaching earth	7.752	3.5	–	–	[40]
Nanoscale aluminum oxide hydroxide	3.259	5.2 ± 0.2	298	–	[41]
NH_2–Fe_3O_4	22.523	2	298	Langmuir	This
NH_2–Fe_3O_4	47.393	2	303		study
NH_2–Fe_3O_4	52.91	2	313		

Table 4
Leaching of Fe ions after re-suspending the MNPs–NH_2 laden with fluoride in deionized water for 6 d

Time (d)	Fe (ng mL^{-1})
0.5	2.601
1	3.652
2	7.959
3	10.28
4	11.31
5	14.68
6	17.62

in the structure and magnetic property of Fe_3O_4 cores. The effects of controlling parameters, such as contact time, temperature, pH, adsorbent dose (Fe_3O_4–NH_2), and initial concentration of fluoride, were studied, as well. Based on the findings, the best dose of Fe_3O_4–NH_2 was 0.4 g/L at the fluoride concentration of 3 mg/L, and the maximum adsorption of fluoride ions was found at pH of 2 and temperature of 313°K. Additionally, the best contact time was 30 min. The equilibrium data were applied using the Freundlich and Langmuir isotherm models. The results showed that the sorption of fluoride ions was well fitted to the Langmuir isotherm, with the maximum fluoride sorption capacity of 22.52–52.91 mg g^{-1} at 298°K–313°K. Moreover, Fe_3O_4–NH_2 could remove about 76.8% of fluoride from aqueous solutions. Therefore, Fe_3O_4–NH_2 could be quickly separated with an external magnet and could be regarded as a potential candidate for fluoride ions removal from aqueous solutions.

Acknowledgments

This research was supported by Center for Water Quality Research (CWQR), Institute for Environmental Research (IER) (grant No. 94-01-46-28628). Hereby, the authors would like to thank Tehran University of Medical Sciences, School of Public Health, for their cooperation. They are also grateful to Ms. A. Keivanshekouh at the Research Improvement Center of Shiraz University of Medical Sciences for improving the use of English in the manuscript.

References

[1] E. Kumar, A. Bhatnagar, U. Kumar, M. Sillanpää, Defluoridation from aqueous solutions by nano-alumina: characterization and sorption studies, J. Hazard. Mater., 186 (2011) 1042–1049.
[2] J. Nouri, A.H. Mahvi, A. Babaei, E. Ahmadpour, Regional pattern distribution of groundwater fluoride in the Shush aquifer of Khuzestan County, Iran, Fluoride, 39 (2006) 321–325.
[3] G. Asgari, B. Roshani, G. Ghanizadeh, The investigation of kinetic and isotherm of fluoride adsorption onto functionalize pumice stone, J. Hazard. Mater., 217 (2012) 123–132.
[4] N. Minju, K. Venkat Swaroop, K. Haribabu, V. Sivasubramanian, P. Senthil Kumar, Removal of fluoride from aqueous media by magnesium oxide-coated nanoparticles, Desal. Wat. Treat., 53 (2015) 2905–2914.
[5] S. Dobaradaran, A.H. Mahvi, S. Dehdashti, S. Dobaradaran, R. Shoara, Correlation of fluoride with some inorganic constituents in groundwater of Dashtestan, Iran, Fluoride, 42 (2009) 50–53.
[6] X. Zhao, J. Wang, F. Wu, T. Wang, Y. Cai, Y. Shi, G. Jiang, Removal of fluoride from aqueous media by Fe_3O_4@Al(OH)$_3$ magnetic nanoparticles, J. Hazard. Mater., 173 (2010) 102–109.
[7] L. Lv, Defluoridation of drinking water by calcined MgAl-CO_3 layered double hydroxides, Desalination, 208 (2007) 125–133.
[8] S.-X. Teng, S.-G. Wang, W.-X. Gong, X.-W. Liu, B.-Y. Gao, Removal of fluoride by hydrous manganese oxide-coated alumina: performance and mechanism, J. Hazard. Mater., 168 (2009) 1004–1011.
[9] M. Bhaumik, T.Y. Leswifi, A. Maity, V. Srinivasu, M.S. Onyango, Removal of fluoride from aqueous solution by polypyrrole/Fe_3O_4 magnetic nanocomposite, J. Hazard. Mater., 186 (2011) 150–159.
[10] M.R. Boldaji, A. Mahvi, S. Dobaradaran, S. Hosseini, Evaluating the effectiveness of a hybrid sorbent resin in removing fluoride from water, Int. J. Environ. Sci. Technol., 6 (2009) 629–632.
[11] S. Ghorai, K. Pant, Equilibrium, kinetics and breakthrough studies for adsorption of fluoride on activated alumina, Sep. Purif. Technol., 42 (2005) 265–271.
[12] G.V. Patankar, A.S. Tambe, B.D. Kulkarni, A. Malyshew, S.P. Kamble, Defluoridation of drinking water using PURAL®MG-20 mixed hydroxide adsorbent, Water Air Soil Pollut., 224 (2013) 1–13.

[13] R.L. Ramos, J. Ovalle-Turrubiartes, M. Sanchez-Castillo, Adsorption of fluoride from aqueous solution on aluminum-impregnated carbon, Carbon, 37 (1999) 609–617.
[14] A. Salifu, B. Petrusevski, K. Ghebremichael, L. Modestus, R. Buamah, C. Aubry, G. Amy, Aluminum (hydr)oxide coated pumice for fluoride removal from drinking water: synthesis, equilibrium, kinetics and mechanism, Chem. Eng. J., 228 (2013) 63–74.
[15] J. Zhang, S. Zhai, S. Li, Z. Xiao, Y. Song, Q. An, G. Tian, Pb(II) removal of Fe_3O_4@SiO_2–NH_2 core–shell nanomaterials prepared via a controllable sol–gel process, Chem. Eng. J., 215 (2013) 461–471.
[16] J.-M. Zhang, S.-R. Zhai, B. Zhai, Q.-D. An, G. Tian, Crucial factors affecting the physicochemical properties of sol–gel produced Fe_3O_4@SiO_2–NH_2 core–shell nanomaterials, J. Sol-Gel Sci. Technol., 64 (2012) 347–357.
[17] N. Kabay, Ö. Arar, S. Samatya, Ü. Yüksel, M. Yüksel, Separation of fluoride from aqueous solution by electrodialysis: effect of process parameters and other ionic species, J. Hazard. Mater., 153 (2008) 107–113.
[18] Y. Tan, M. Chen, Y. Hao, High efficient removal of Pb(II) by amino-functionalized Fe_3O_4 magnetic nano-particles, Chem. Eng. J., 191 (2012) 104–111.
[19] J. Aguado, J.M. Arsuaga, A. Arencibia, M. Lindo, V. Gascón, Aqueous heavy metals removal by adsorption on amine-functionalized mesoporous silica, J. Hazard. Mater., 163 (2009) 213–221.
[20] Y.-M. Hao, C. Man, Z.-B. Hu, Effective removal of Cu(II) ions from aqueous solution by amino-functionalized magnetic nanoparticles, J. Hazard. Mater., 184 (2010) 392–399.
[21] S.-H. Huang, D.-H. Chen, Rapid removal of heavy metal cations and anions from aqueous solutions by an amino-functionalized magnetic nano-adsorbent, J. Hazard. Mater., 163 (2009) 174–179.
[22] O. Sayar, M.M. Amini, H. Moghadamzadeh, O. Sadeghi, S.J. Khan, Removal of heavy metals from industrial wastewaters using amine-functionalized nanoporous carbon as a novel sorbent, Microchim. Acta, 180 (2013) 227–233.
[23] H. Shen, S. Pan, Y. Zhang, X. Huang, H. Gong, A new insight on the adsorption mechanism of amino-functionalized nano-Fe_3O_4 magnetic polymers in Cu(II), Cr(VI) co-existing water system, Chem. Eng. J., 183 (2012) 180–191.
[24] L. Wang, J. Bao, L. Wang, F. Zhang, Y. Li, One-pot synthesis and bioapplication of amine-functionalized magnetite nanoparticles and hollow nanospheres, Chem. Eur. J., 12 (2006) 6341–6347.
[25] Y.-G. Zhao, H.-Y. Shen, S.-D. Pan, M.-Q. Hu, Q.-H. Xia, Preparation and characterization of amino-functionalized nano-Fe_3O_4 magnetic polymer adsorbents for removal of chromium(VI) ions, J. Mater. Sci., 45 (2010) 5291–5301.
[26] J. Watson, B. Cressey, A. Roberts, D. Ellwood, J. Charnock, A. Soper, Structural and magnetic studies on heavy-metal-adsorbing iron sulphide nanoparticles produced by sulphate-reducing bacteria, J. Magn. Magn. Mater., 214 (2000) 13–30.
[27] J. Chen, Y. Hao, M. Chen, Rapid and efficient removal of Ni^{2+} from aqueous solution by the one-pot synthesized EDTA-modified magnetic nanoparticles, Environ. Sci. Pollut. Res., 21 (2014) 1671–1679.
[28] A.N. Baghani, A.H. Mahvi, M. Gholami, N. Rastkari, M. Delikhoon, One-Pot synthesis, characterization and adsorption studies of amine-functionalized magnetite nanoparticles for removal of Cr(VI) and Ni(II) ions from aqueous solution: kinetic, isotherm and thermodynamic studies, J. Environ. Health Sci. Eng., 14 (2016) 1.
[29] M. Ghoul, M. Bacquet, G. Crini, M. Morcellet, Novel sorbents based on silica coated with polyethylenimine and crosslinked with poly (carboxylic acid): preparation and characterization, J. Appl. Polym. Sci., 90 (2003) 799–805.
[30] R. Gulati, R. Saxena, R. Gupta, Fermentation waste of *Aspergillus terreus*: a potential copper biosorbent, World J. Microbiol. Biotechnol., 18 (2002) 397–401.
[31] X. Guo, B. Du, Q. Wei, J. Yang, L. Hu, L. Yan, W. Xu, Synthesis of amino functionalized magnetic graphenes composite material and its application to remove Cr(VI), Pb(II), Hg(II), Cd(II) and Ni(II) from contaminated water, J. Hazard. Mater., 278 (2014) 211–220.
[32] Y.G. Zhao, H.Y. Shen, M.Q. Hu, F. Wei, Y.J. Luo, Q.H. Xia, Synthesis of NH_2-functionalized nano-Fe_3O_4 magnetic polymer adsorbent and its application for the removal of Cr(VI) from industrial wastewater, Adv. Mat. Res., 79–82 (2009) 1883–1886.
[33] A. Jamode, V. Sapkal, V. Jamode, Defluoridation of water using inexpensive adsorbents, J. Indian Inst. Sci., 84 (2004) 163–171.
[34] R. Bhaumik, N. Mondal, B. Das, P. Roy, K. Pal, C. Das, A. Baneerjee, Eggshell powder as an adsorbent for removal of fluoride from aqueous solution: equilibrium, kinetic and thermodynamic studies, J. Chem., 9 (2012) 1457–1480.
[35] A. Tembhurkar, S. Dongre, Studies on fluoride removal using adsorption process, J. Environ. Sci. Eng., 48 (2006) 151–156.
[36] M. Najafi, Y. Yousefi, A. Rafati, Synthesis, characterization and adsorption studies of several heavy metal ions on amino-functionalized silica nano hollow sphere and silica gel, Sep. Purif. Technol., 85 (2012) 193–205.
[37] D.K. Malay, A.J. Salim, Comparative study of batch adsorption of fluoride using commercial and natural adsorbent, Res. J. Chem. Sci., 1 (2011) 68–75.
[38] B.M. Mamilwar, A. Bhole, A. Sudame, Removal of fluoride from ground water by using adsorbent, Int. J. Eng. Res. Appl., 2 (2012) 334–338.
[39] A. Daifullah, S. Yakout, S. Elreefy, Adsorption of fluoride in aqueous solutions using $KMnO_4$-modified activated carbon derived from steam pyrolysis of rice straw, J. Hazard. Mater., 147 (2007) 633–643.
[40] M. Mahramanlioglu, I. Kizilcikli, I. Bicer, Adsorption of fluoride from aqueous solution by acid treated spent bleaching earth, J. Fluorine Chem., 115 (2002) 41–47.
[41] S.G. Wang, Y. Ma, Y.J. Shi, W.X. Gong, Defluoridation performance and mechanism of nano-scale aluminum oxide hydroxide in aqueous solution, J. Chem. Technol. Biotechnol., 84 (2009) 1043–1050.